



Striking Perturbations of Ionospheric Total Electron Content (TEC) During Earthquake

Najat M.R. Al-Ubaidi*, Isra'a A. Mohammed Ali

Department of Astronomy and Space, College of Science, University of Baghdad, Baghdad, Iraq

*najatmr10@yahoo.com

Abstract

To study the striking perturbations of ionospheric Total Electron Content (TEC) before, during, and after the earthquake ($M \geq 5$) for earlier prediction to avoid calamities, ionospheric TEC data are taken by using red shift technique from two-frequencies GPS signals.. Tohoku earthquake on 11th March 2011 is chosen as case of our study (A magnitude M9.0 earthquake reported by the US Geological Survey gives its origin time at 05:46:23 UTC; the epicenter was located at 38.322°N, 142.369°E of the east coast of Honshu). The study was made 15 days before and 15 days after earthquake occurred over Japan at four different geographic positions, Kokubunji (35.7°N, 139.5°E), Wakkanai (45.2°N, 141.8°E), Yamagawa (31.2°N, 130.6°E) and Okinawa (26.7°N, 128.2°E). Observations TEC values compared with predicted TEC values by using the International Reference Ionosphere (IRI 2007) model to study the accuracy of model during the earthquake. Finally absolute error calculated between observed TEC (Obs.) values and predicted (Pre.) values before and after correction for 24 hours, which is reveals fewer errors after correction.

Keywords: Ionosphere; Earthquake; TEC; IRI2007 model.

الاضطرابات الحاصلة في طبقة الايونوسفير للمحتوى الالكتروني TEC اثناء الزلزال

نجاة محمد رشيد رؤوف العبيدي* , إسراء عبد القاسم محمد علي

قسم الفلك والفضاء, كلية العلوم, جامعة بغداد, بغداد, العراق

الخلاصة

لدراسة الاضطرابات الحاصلة في الطبقات العليا من الايونوسفير وللمحتوى الالكتروني (TEC) قبل وأثناء وبعد وقوع الزلازل والتي هي بدرجة ($M \leq 5$) والتنبأ بها قبل حدوثها وذلك تجنباً لحدوث الكوارث الطبيعية، تم اختيار البيانات من جهاز التعقب الارضي ولترددتين مختلفتين وبطريقة ازاحت دوبلر لحساب المحتوى الالكتروني ولارتفاعات مختلفة. زلزال توهوكو (والذي كان بدرجة M 9.0 والمسجل من قبل هيئة المسح الجيولوجي الامريكية وان وقت حدوث الزلزال كان الساعة 5:46:23 UTC ويقع مركز الزلزال على خط عرض 38.322N، وخط طول 142.369E من الساحل الشرقي لمدينة (Honshu) وفي يوم 11 مارس من عام 2011) كحالة لهذه الدراسة. وأخذت البيانات من اربعة مواقع جغرافية مختلفة وهي Kokobunji (35.7N, 139.5E), Wakkanai (45.2N, 141.8E), Yamagawa (31.2N, 130.6E), Okinawa (26.7N, 128.2E) لقيم المحتوى الالكتروني TEC الأيونوسفيرية. وقد أجريت هذه الدراسة قبل 15 يوماً وبعد 15

وما من وقوع الزلزال. إجريت مقارنة بين القيم الملاحظة والقيم المتوقعة والمحسوبة من الامتداد العالمي IRI2007 وذلك لدراسة مدى دقة هذا الامتداد خلال الزلزال. وتم حساب الخطأ بين القيم المرصودة والقيم المتوقعة قبل وبعد التصحيح وجد بان الخطأ اقل بعد التصحيح.

1. Introduction

The ionosphere has a significant contribution in the propagation of electromagnetic radio waves. Such propagations are widely affected due to large variability in the ionosphere. This variability's occur mostly under the influence of some well known geophysical phenomena, namely sunspot numbers, solar flares and magnetic storms. Interestingly, it has been reported that the ionosphere also shows anomalous perturbations prior to the large magnitude earthquakes. The study of ionospheric disturbances during seismic activities has become an interesting field among the scientists working in the field of earthquake prediction. These studies are being carried out by observing different ionospheric parameters, mainly greatest plasma frequency in the ionospheric F2 layer (foF2), critical frequency of the E-layer (foEs), and total electron content (TEC), etc [1].

Recent studies on the ionospheric anomalies before earthquakes indicated the existence of the ionospheric precursors. A large number of reports and publications brought more and more interests focused on the relation between the seismic activity and the ionospheric variability. The physical mechanisms are proposed to testify this relationship and the pre-earthquake ionospheric anomaly. There are two major potential mechanisms which are contributed to the origin of the seismic ionospheric perturbations. One is that the anomalous vertical electric field near the Earth's surface within the radius of the seismogenic zone will penetrate into the ionosphere and cause the irregularities of electron density formation by the ion drifting. The other is that the atmospheric gravity waves (AGW) produced by earthquakes may propagate upward to perturb the ionosphere of earthquakes. These studies have been carried out both by using ground-based techniques and by using satellites. However, the perturbations differ from case to case and current large day-to-day variability [2].

This paper focus on the disturbances of ionospheric TEC during the March 11 earthquake, using data from dual frequency GPS receivers around epicenter of earthquake which can be regarded as short term earthquake

precursor as a way to predict earthquake after eliminating ionospheric anomalies that may be caused by solar activities or geomagnetic storms.

2. Total Electron Content (TEC)

TEC defined as the total number of electrons integrated along the path from the GPS satellite (S) to receiver (R). TEC as an indicator of ionospheric variability that derived by the modified GPS signal through free electrons. It also the parameter of the ionosphere that produces most of the effects on GPS signals. A value of TEC equal to 10^{16} electrons.m⁻² is called one TEC Unit (TECU) which is determined as below [3, 4]:

$$TEC = \int_R^S N_e \cdot dr \quad (1)$$

N_e = Local electron density (electron.m⁻³),
 dr = Distance travelled by the signal.

Slant and Vertical TEC

Slant total electron content (TECs) is a measure of the total electron content of the ionosphere along the ray path from the satellite to the receiver, as in Figure 1. Vertical total electron content (TEC_v) enables TEC to be mapped across the surface of the Earth. The TECs, from equation (1) can be calculated using GPS two different radio wave signals by using Doppler shift [5]

$$TEC_s = \frac{\Delta p}{40.3} \left(\frac{f_1^2 f_2^2}{f_1^2 - f_2^2} \right) \quad (2)$$

Where Δp is the difference between time delays measured by the L1 and L2 waves, f_1 (1575.42 MHz) is the frequency of the L1 wave and f_2 (1227.6 MHz) is the second frequency of the L2 wave.

Equation (3) is to convert TECs to vertical TEC

$$TEC_v = TEC_s \cos(z') \quad (3)$$

$$\cos(z') = \sqrt{1 - \sin^2(z)} \quad (4)$$

$$\sin(z') = \frac{R_e}{R_e + H} \sin(z) \quad (5)$$

Where R_e = Mean Earth radius, 6371 km, H = maximum height of electron density, 350 km, z

= zenith angle at the receiver site and $z' = (90^\circ - z)$ is the zenith angle at the ionospheric Pierce Point (IPP) [6].

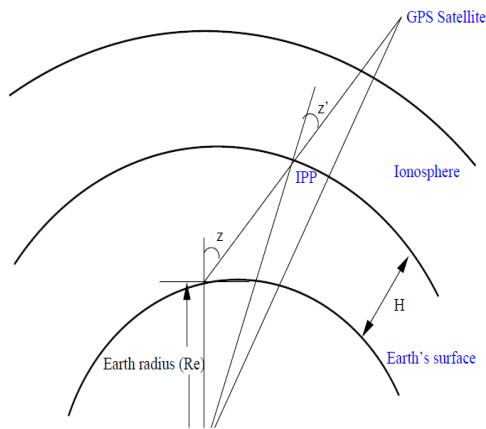


Figure 1- Geometry of Satellite-Receiver Link.

- **Dst index**

The Dst (Disturbance Storm Index) is a measure of geomagnetic activity used to assess the severity of magnetic storms. It is expressed in nanoteslas and is based on the average value of the horizontal component of the Earth's magnetic field [7]. Negative Dst values indicate a magnetic storm is in progress, the more negative Dst is the more intense the magnetic storm. The negative deflections in the Dst index are caused by the storm time ring current which flows around the Earth from east to west in the equatorial plane. The ring current results from the differential gradient and curvature drifts of electrons and protons in the near Earth region and its strength is coupled to the solar wind conditions. Only when there is an eastward electric field in the solar wind which corresponds to a southward interplanetary magnetic field (IMF) is there any significant ring current injection resulting in a negative change to the Dst index. Thus, by knowing the solar wind conditions and the form of the coupling function between solar wind and ring current, an estimate of the Dst index can be made [8].

- **$F_{10.7}$ Index**

The Sun emits radio energy with normally slowly varying intensity. This radio flux changes from day to day seemingly in response to the number of spot groups on the disk. Solar flux from the entire disk has been routinely recorded at a frequency of 2800 MHz by radio telescopes at the Algonquin Radio Observatory in Ottawa

[9]. $F_{10.7}$ is considered as an indicator of the overall solar activity. It correlates well with the sunspot number as well as with the solar extreme ultraviolet radiation, which controls the ionospheric conductivity. The observed values are adjusted for the changing sun-earth distance and for uncertainties in antenna gain [10].

4. International Reference Ionosphere (IRI) Model

The IRI is an international project sponsored by the Committee on Space Research (COSPAR) and the International Union for Radio Science (URSI). For a given geographic location, time and date, the IRI model describes the electron density, electron temperature, ion temperature and ion composition (O^+ , H^+ , He^+ , NO^+ , O_2^+), ion drift and Total Electron Content (TEC) in the altitude range 50 – 2 000 km. IRI provides monthly averages in the non-auroral ionosphere for magnetically quiet conditions. The major data sources for the IRI model development are the world-wide 16 network of ionosondes, incoherent scatter radar, satellite top side sounders and in situ instruments on several satellites and rockets [11].

5. Data Selection and Analyses

In this research, the data of ionospheric TEC were taken using two-frequencies GPS signals transmitted from satellites at about 20,000 km above the Earth at an inclination angle of 55° and recorded by ground GPS receivers (GEONET, consisting of more than 1,200 stations with 300 km altitude). It operated by the Geospatial Information Authority of Japan (GSI) for four locations at different geographic positions, Kokubunji ($35.7^\circ N$, $139.5^\circ E$), Wakkanai ($45.2^\circ N$, $141.8^\circ E$), Yamagawa ($31.2^\circ N$, $130.6^\circ E$) and Okinawa ($26.7^\circ N$, $128.2^\circ E$) as in Table.1, which is listed the locations and distances from the epicenter to the different geographic mid-latitude positions in Japan region, this data taken during the last strong Tohoku earthquake (A magnitude M9.0 earthquake which is reported by the U.S. Geological Survey gives its origin time at 05:46:23 UTC; the epicenter was located at $38.322^\circ N$, $142.369^\circ E$ off the east coast of Honshu) on 11th March 2011. The study was made 15 days before and 15 days after the earthquake occurred, which is from 24th February 2011 until 26th March 2011, Figure 2 illustrates locations of the epicenter with four

different geographic positions in Japan. Also, it is known the detection of seismo-ionospheric effects is rather complicated in the periods of solar and geomagnetic disturbances. Ionospheric modification caused by geomagnetic storm activity can promote amplification or weakening of the seismo-ionospheric effects manifestation. Figure 3 shows the daily variations of solar and geomagnetic indices ($F_{10.7}$ and Dst indices) respectively for the period from February 24 to March 26. By using the International Reference Ionospheric (IRI2007) model to predict the values of TEC during the same days of earthquake occurred to find the accuracy of this model during the earthquake. Because there is nonlinear correlation between the observed and predicted values along the day (24 hours), so correction between the observed and predicted values can be made using equation (6) bellow

$$Corr = a_0 + a_1 T + a_2 T^2 \quad (6)$$

Where, Corr mean the corrected TEC values with local time (T) which is taken for 24 hours all the day. The coefficients a_0 , a_1 , and a_2 represent the parameters results from curve fitting.

Table 1 - Locations and distances to epicenter

Locations	Distance(km)
Wakkanai (45.2°N, 141.8°E)	769
Kokubunji (35.7°N, 139.5°E)	387
Yamagawa (31.2°N, 130.6°E)	1,334
Okinawa(26.7°N, 128.2°E)	1,850

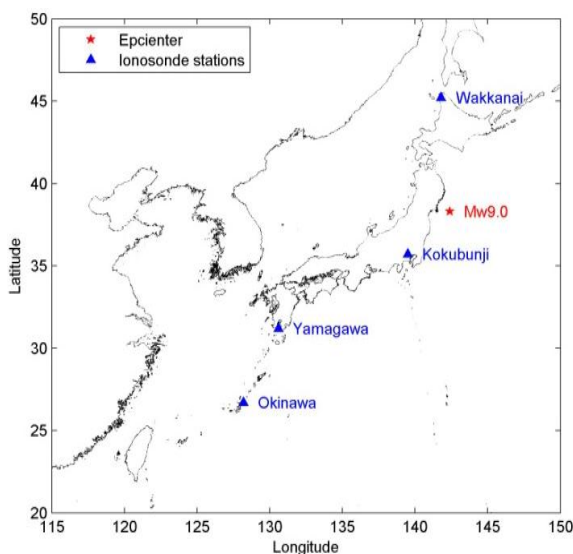


Figure 2- Locations of the epicenter with different geographic position

6. Results and Discussion

In our study ionospheric disturbances were examined before, during, and after Tohoku earthquake of March 11, 2011. For this event we have considered TEC over four different geographic locations around the epicenter of earthquake in Japan. Figures 4,5,6,7 show the diurnal variations of TEC with local time Japan Standard Time (JST), from February 24 to March 24 (15 days before and 15 days after the earthquake) for four locations chosen in this research Kokobunji, Wakkanai, Yamagawa, and Okinawa respectively. Figure 4, for Kokobunji location which is the closest station to the epicenter see Figure 2, which indicates that the instability of TEC was detected on March 2-3 and significant abnormal on March 8 (3 days before the earthquake). The instability of TEC was continued several days after the day of earthquake until reached to the quite stable value which is on 26th March. Figure 5 represents the results for Wakkanai location which encompasses the earthquake event during the same days. In this figure there were some abnormal on March 2-3 and striking disturbances on March 7-8 (4 or 3 days prior to earthquake). The values of TEC increased on the day of earthquake and for one day afterward, then returned to normal condition on March 13 and continued until March 26 except March 23-24. Figure 6 shows 31-day over Yamagawa location. The results are similar to the Kokobunji station. Also, the disturbances of TEC appeared on the day of earthquake and for 2 days after it, then to normal condition on March 16 and continued until March 26. Figure7, results over Okinawa location during the period around the earthquake. The coordinates of Okinawa is 26.68°N, 128.15°E, which is 10° south of the epicenter. It is clear from this figure there were some enhancement anomalies on March 1-3 and striking disturbance on March 8 like other figures in which the values of TEC were clearly larger than other days. The disturbances of TEC went up on the day of earthquake and continued until March 16 after that, stabled in the other days except from 19 March till 21 March.

Figure 3 shows the solar and geomagnetic indices, $F_{10.7}$ indices were above 100 during March 1-15 and reached 155 on March 8 (pre the earthquake) and March 21-26, indicating strong solar radiation. There were geomagnetic disturbances on March 1-2 and March 10-12

($Dst < -40$ nT). The geomagnetic field on the other days was low ($Dst > -20$). We analyzed the causes of the ionospheric anomalies before the earthquake, and attempted to exclude anomalies that may have been caused by solar or geomagnetic activities. During March 1-2, the Dst index reached -61 nT indicating the likelihood of a geomagnetic storm on these 2 days. Therefore, we believe that the ionospheric anomalies on these 2 days were caused by solar activity and a magnetic storm. On March 8 the values of TEC from the four stations showed significant and persistent positive anomalies. From Figure 3 in March 8, Dst was greater than -20 nT, thus the geomagnetic field was very quiet. However, the $F_{10.7}$ index on March 8 reached 155 signifying the strongest solar radiation of the period. There was a certain relationship between the ionospheric anomalies and the intense solar activity. Therefore, further analysis is needed to determine whether the ionospheric anomalies on March 8 were caused

by the earthquake or solar activities (which will be published later in other paper). There were also ionospheric anomalies during March 11–13. Nevertheless, solar and geomagnetic field activities were intense during these days, and we consider these anomalies to be caused by solar and geomagnetic field activities. The results which is obtained from the model reveals that there is no correlation between the observed and predicted values during the earthquake period, so correction made to the model. Finally, by using equation bellow

$$\text{Absolute error} = \sqrt{(\text{Obs.} - \text{Pre.})^2} \quad (7)$$

We can find the absolute error between observed TEC (Obs.) values and predicted (Pre.) values before and after correction for 24 hours as in Appendix, which is reveals less errors after correction.

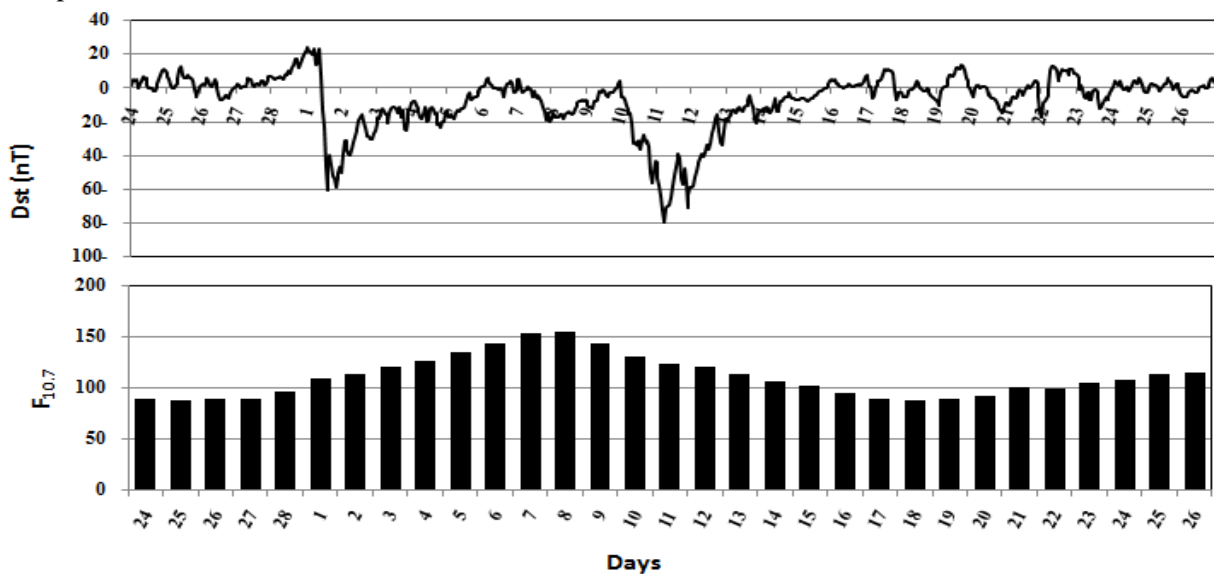


Figure 3- Solar and geomagnetic conditions during the earthquake period.

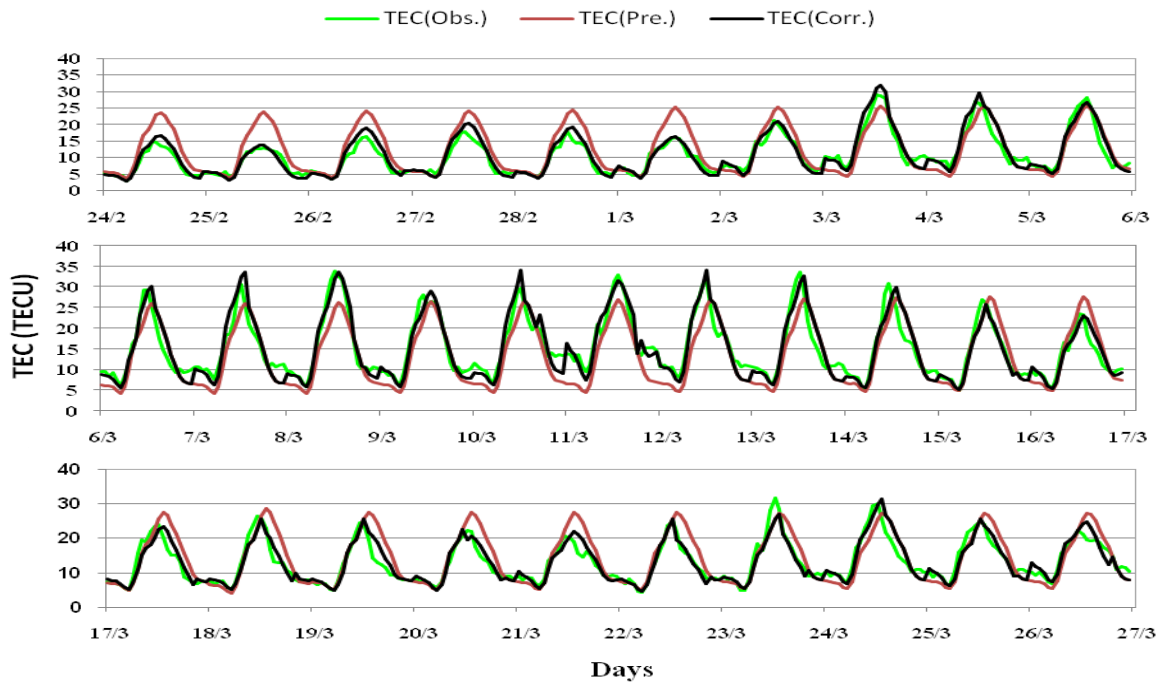


Figure 4 - Diurnal variations of TEC with local time at Kokobunji station, from February 24 to March 26 (15 days before and 15 days after earthquake).

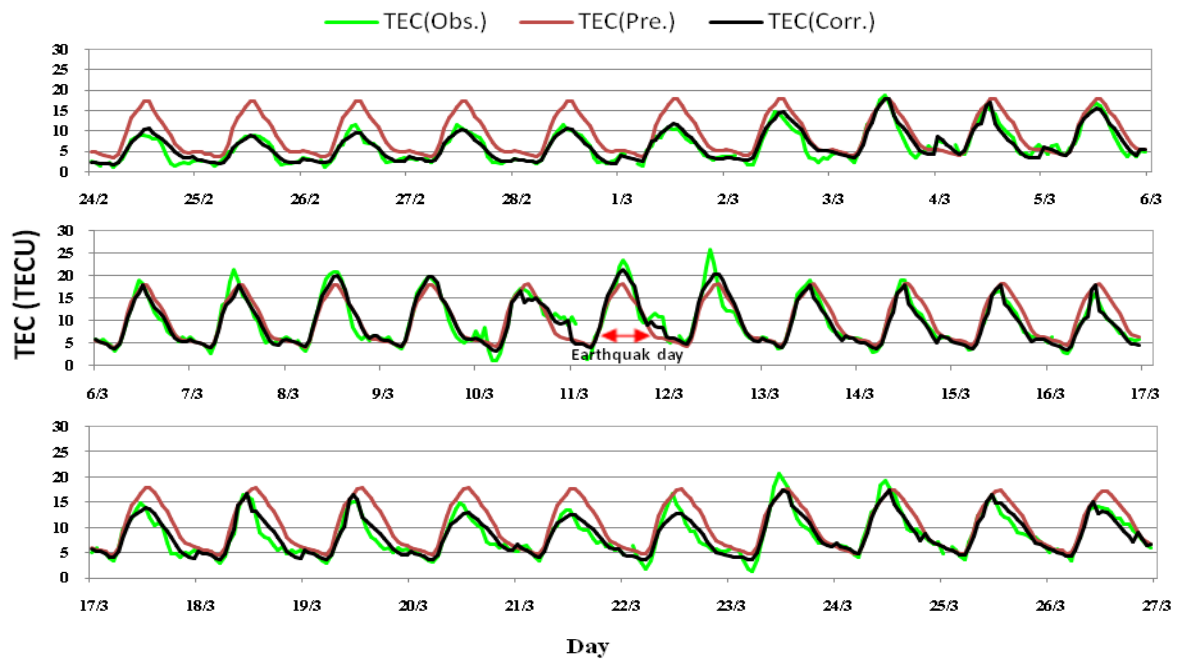


Figure 5- Diurnal variations of TEC with local time at Wakkanai, from February 24 to March 26 (15 days before and 15 days after earthquake).

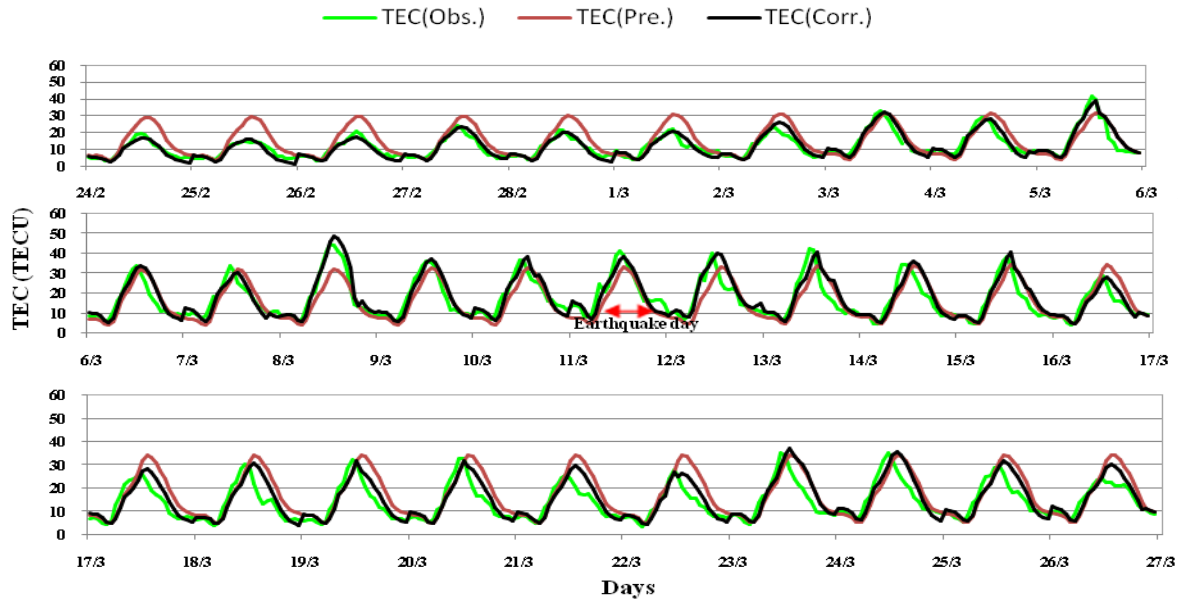


Figure 6- Diurnal variations of TEC with local time at Yamagawa, from February 24 to March 26 (15 days before and 15 days after earthquake).

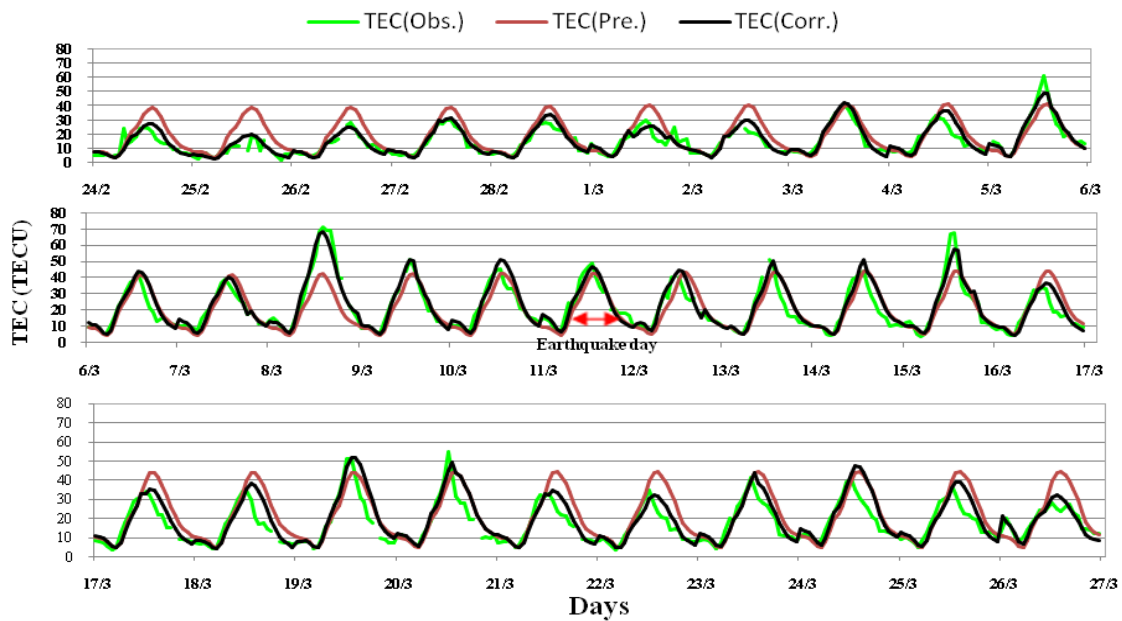


Figure7- Diurnal variations of TEC with local time at Okinawa, from February 24 to March 26 (15 days before and 15 days after earthquake).

7. Conclusions

Our study shows that similar pre-earthquake ionospheric anomalies can be found in the TEC several days before the earthquake for four stations around epicenter of earthquake. After analyzing the diurnal variation of TEC, we believe that the positive anomalies on March 8

are a likely seismo-ionospheric precursor of the earthquake.

It is believed that these undetermined seismic-ionospheric anomalies may have a close relationship with the enhanced emission of infrared radiations from the epicenters. It is possible that the radon emanating from the crust within the seismically active areas produces the

air ionization. The heavy charged ion clusters raise in the troposphere and lead to the vertical electric field providing the electrodynamic coupling between the ground and ionosphere a few days before earthquakes. The anomalous vertical electric field penetrates into the ionosphere which would affect the variations of the ionospheric densities.

Acknowledgement

Authors are thankful to the Geospatial Information Authority of Japan, for providing the GPS data. WDC Kyoto Japan for providing the data of dst index and WDC UK, for $F_{10.7}$ index data.

References

1. Singh V., Chauhan V., Singh O. P. and Singh B., **2010**, Ionospheric effect of Earthquakes as determined from ground bases TEC measurement and satellite data, Indian journal of radio and space physics, Vol. **39**, pp. 63-70.
2. Xia C., Wang Q., Yu T., Xu G., Yang S., **2011**, Variations of ionospheric total electron content before three Strong Earthquakes in the Qinghai-Tibet region, Advances in space research, Vol. **47**, pp. 506–514.
3. Ya'acob N., Abdullah M., Ismail M., Zaharim A., **2009**, Model Validation for GPS Total Electron Content (TEC) using 10th Polynomial Function Technique at an Equatorial Region, WSEAS TRANSACTIONS On COMPUTERS, Vol. **8**, pp. 1533-1542, ISSN: 1109-2750.
4. Spits J., **2012**, Total Electron Content reconstruction using triple frequency GNSS signals, Ph.D., Thesis, Faculty of Sciences, Department of Geography, Universite de Liege.
5. Ya'acob N., Jusoh M. H., Member, IEEE, Abdullah M. and Ismail M., Senior Member, IEEE, December **2007**, Monitoring the TEC Variation Using GPS Dual Frequency System During Quiet and Disturbed Day, The 5th Student Conference on Research and Development –SCORED 2007, 11-12, Malaysia.
6. Jusoh M. H., Jusoh N. h., Othman N., Haron M. A., Saad H., 26-27 October **2009**, Determination of Optimized Ionospheric Layer for TEC Measurement at Equatorial Region, Proceeding of the International Conference on Space Science and Communication, , Port Dickson, Negeri Sembilan, Malaysia
7. pluto.space.swri.edu/IMAGE/glossary/dst.html.
8. Mubarak W. A., Abdullah M., Misran N., **2009**, Ionospheric TEC response over Simeulue earthquake of 28 March 2005, Proceeding of the 2009 International Conference on Space Science and Communication, 26-27 October 2009, Port Dickson, Negeri Sembilan, Malaysia.
9. Perrone L. and Franceschi G. D., **1998**, Solar, ionospheric and geomagnetic indices, Annali di geofisica, Vol. **41** pp. 5–6.
10. Verbanac G., Manda M., Vršnak B., and Sentic S., **2011**, Evolution of Solar and Geomagnetic Activity Indices, and Their Relationship: 1960 – 2001, Solar Phys, Vol. **271** pp. 183–195.
11. Opperman B., **2007**, Reconstructing Ionospheric TEC over South Africa Using Signals from a Regional GPS Network, Ph.D., thesis, Rhodes University.